Texture analysis of images using Principal Component Analysis

Manish H. Bharati, John F. MacGregor*

Dept. of Chem. Eng., McMaster University, Hamilton, Ont., Canada, L8S 4L7

ABSTRACT

Extracting texture/roughness information from grayscale or multispectral images for off-line quality control, or on-line feedback control is a difficult problem. Several statistical, structural & spectral texture analysis approaches for grayscale images (using various pre-defined filters etc.) have been suggested in the literature[1, 2]. In this paper we propose a new approach based on Multivariate Image Analysis techniques using multi-way Principal Component Analysis. Prior to analysis the grayscale images are transformed into three-dimensional pixel intensity arrays through spatial shifting of the image in several directions followed by stacking the shifted images on top of each other. The resulting three-dimensional image data is a multivariate image where the third (i.e. variable) dimension is the spatial shifting index. Multi-way PCA is then used to extract features (PC scores), which contain the greatest amount of variation. Plots of the observed values of these scores against one another define a score space. Certain regions of this score space contain the texture information of the grayscale image. By masking these regions and tracking the number of pixels having features that fall in these regions, or by comparing the score spaces with template exemplars, one is able to monitor changes in the image surface textural properties. The approach is illustrated using a set of grayscale images of the surface of steel sheet. Based on the textural features extracted from the surface images a simple classification scheme is devised in which each sample image is assigned into one of two classes representing good or bad surface characteristics.

Keywords: Multivariate Image Analysis, Principal Component Analysis, Texture Analysis, Image Classification

1. INTRODUCTION

Although image texture is not very well defined in the literature, one can intuitively describe several image properties such as smoothness, coarseness, depth etc. with texture. Russ[3] loosely defines image texture as a descriptor of the local brightness variation from pixel to pixel in a small neighborhood through an image. If the image can be represented as a two-dimensional surface upon which each pixel represents a square column, then the pixel intensity (i.e. brightness) could be described by the elevation of each column in a three-dimensional histogram. As the adjacent pixel brightness variation in an image increases, the surface of the three-dimensional histogram becomes less smooth. Image texture can give a quantitative measure of the degree of surface roughness in an image. In traditional image processing literature there are primarily three different approaches used to describe the texture of a region in an image. The three approaches are *statistical*, *structural*, and *spectral* texture analysis. Statistical texture analysis techniques primarily describe texture of regions in an image through moments of its grayscale histogram. According to the number of pixels defining the local region (i.e. feature), statistics can be divided into first, second, or higher moments of the grayscale histogram[4]. Using statistical analysis one can characterize textures as smooth, coarse, grainy etc. Furthermore, statistics of some local geometrical features such as edges, peaks, valleys, blobs etc. can also give measures of specific texture properties in an image. On the other hand, structural texture analysis techniques decompose a pattern in an image into texture elements (e.g. description of interlocked bricks in an image using regularly spaced parallel lines). In structural analysis the properties and placement rules of the texture elements define the texture[4]. Finally, spectral texture analysis techniques are based on the properties of the Fourier spectrum of an image. Fourier transforms detect global periodicity in images, producing high-energy peaks in their spectrum at those wavelengths that describe the major periodic components in the pixel brightness throughout the image.

Each of the three texture analysis approaches described above have their own merits. Depending upon the type of information sought, one can apply the appropriate technique to gather a more quantitative measure of the texture property in an image. In this paper we describe a new multivariate statistical texture analysis method using Multivariate Image Analysis (MIA) techniques, which are based on multi-way Principal Component Analysis (PCA). Image data when collected in

* Correspondence: Email: macgreg@mcmaster.ca; WWW: http://chemeng.mcmaster.ca/faculty/macgregor; Tel: 905 525 9140 x 24951; Fax: 905 521 1350

multiple variables (e.g. spectra) forms a three-dimensional data set, where the third dimension (orthogonal to the 2D image plane) represents the variables. Such multivariate image data consists of a stack of congruent images, where each pixel location in the image plane is represented by multiple brightness values. As a result, there is an enormous amount of highly correlated data in multivariate images. MIA techniques have previously been shown to successfully analyze multivariate image data[5, 6, 7.] This is accomplished by compressing the highly correlated data into a reduced dimensional subspace through a few linear combinations (generally lower than the number of variables in the multivariate image) of the brightness values per pixel location in the image plane. A 3-way data matrix $\underline{\mathbf{X}}$ can generally represent the three-dimensional pixel intensity data of a multivariate image. Upon performing a multi-way PCA decomposition on $\underline{\mathbf{X}}$ one can represent the multivariate image in a subspace, called the Latent Variable (LV) space of MIA, as follows:

$$\underline{\mathbf{X}} = \sum_{a=1}^{A} \mathbf{T}_a \otimes \mathbf{p}_a + \underline{\mathbf{E}} \tag{1}$$

where $\mathbf{T}$, $\mathbf{P}$, and $\underline{\mathbf{E}}$ are the score, loading, and residual matrices of the LV space, respectively. The Kronecker product between a matrix and a vector is represented by $\otimes$. Generally, A is lower than the variable dimension of $\underline{\mathbf{X}}$. The main advantage of MIA lies in its ability to *visually* illustrate the score vectors (columns of $\mathbf{T}$, i.e. $\mathbf{t}_a$), upon reorganization into a two-way array, as individual images $\mathbf{T}_a$ (*image space*). Furthermore, MIA also allows one to view pairs (or triplets) of score vectors as point clusters of scatter plots (*score space*). The inherent duality between the score and image spaces forms the backbone of MIA. One of the main ideas behind this type of image analysis is to isolate pixels belonging to similar features throughout an image, regardless of their spatial locations. This task is simplified by multi-way PCA, as it captures the unique signatures of those pixels belonging to the same feature in a multivariate image and assigns them a specific combination of score values. As a result, pixels belonging to the same features form point clusters upon scatter plotting the score vectors (i.e. score space of MIA). One can investigate individual point clusters in the score space through manual masking (using a mouse and cursor technique), and highlighting the corresponding masked pixels in the image space of MIA. The duality between the image and score space of MIA can be used to isolate and model all features of interest throughout the image. The corresponding model can then be used to analyze new multivariate image data in order to detect and isolate further occurrences of the modeled features. Thus, MIA can be used both as an image analysis as well as monitoring tool.

This paper describes a particular application of MIA techniques specifically for purposes of image texture analysis. Hence, theoretical details of MIA and multi-way PCA will not be described here. The reader is encouraged to consult MacGregor et. al.[8] to understand the theory of MIA techniques used for analysis and monitoring features of interest from multivariate images.

1.1. Multivariate image analysis of industrial grayscale images

MIA techniques are ideally suited for analyzing multivariate images (i.e. sets of congruent digital images). Each image in such a set represents a unique variable (e.g. individual spectra in a multispectral image) that provides specific information regarding the scene being depicted. However, acquisition of such imagery has a considerable cost associated with it. This is mainly because of the more sophisticated sensors required to acquire images in multiple variables (e.g. spectra). Such sensors are mainly used for off-line analyses in the laboratory, remote sensing, and medical applications (e.g. Magnetic Resonance Imaging, Positron Emission Tomography, Satellite Imaging etc.). However, most common industrial imaging sensors used to monitor process conditions & product qualities are much simpler than these. One of the most popular industrial imaging devices is a grayscale camera (analog or digital). Common vision based systems in most industries acquire grayscale images (static or sequences) for process monitoring.

Direct use of MIA techniques (as described above) on grayscale images is not possible. This is because grayscale image data consists of *one* two-way pixel array (as opposed to multiple arrays in a multivariate image). As a result, these images provide only one measurement for the depicted scene per pixel location. On the other hand, multivariate images contain *several* (information specific) variable images, with each variable transmitting unique information about a scene. Upon applying multi-way PCA on such images, each LV pools the information content from the variable images into a single linear combination. This linear combination is based on the amount of variance explained in the variable pixel intensities per pixel location in the image plane. Using this criterion MIA attempts to logically group information from the variable images to enhance specific features. Since grayscale images only have one variable, all information content (relevant or not) would be given equal importance.

This paper attempts to explore the extraction of textural information from industrial grayscale images using the advantageous features of MIA. To this end, creating a 3rd logical dimension to complement the two-way array of a grayscale image has been explored. The proposed technique tries to enhance the texture (i.e. edge) information of features through spatial shifting of the grayscale image in adjacent directions, followed by stacking the shifted images to create a three-way pixel array. MIA

techniques (as described above) can then be used on the resulting image to extract the texture information. Multivariate image texture analysis and automatic classification of grayscale images from the steel manufacturing industry are used as illustrative examples to explore the potentials of the proposed approach. A brief description of the steel image data and its pre-processing steps are provided in the following section. Multivariate Image Analysis of the resulting three-way image array is carried out in section 3. This section also describes techniques of monitoring texture information in various steel surface images by making use of the duality between their score and image spaces. Finally, section 4 describes an automatic classification scheme for a set of steel surface grayscale image samples. The classification is based on a similarity measure among the score spaces of the image samples.

2. DESCRIPTION OF INDUSTRIAL IMAGE DATA

In the steel manufacturing industry, product quality is maintained using various process monitoring and feedback control techniques. However, human intervention is still required to determine if product quality is maintained over long periods of time. Prior to shipping, steel quality is often checked by performing random checks on steel rolls. This is usually accomplished by cutting sections of a particular roll and performing various tests on the sections to determine if the characteristics of the product meet consumer specifications. One of the indicators of overall product quality is smoothness of the steel surface. As the steel quality declines, it affects the surface properties of the product. This results in a coarser steel surface. The amount and distribution of surface pits on steel are good indicators whether or not steel surface quality has been compensated. Deteriorated steel quality affects the number and severity of pits that form on its surface. Good quality steel surfaces have very few pits that are quite shallow and are randomly distributed. These surface pits become deeper and more pronounced in poor steel quality. The point when pits start to join and result in deep craters throughout the steel indicates a coarser surface, which results in bad product. Skilled operators visually determine the degree of steel surface pitting. These operators usually grade the steel based on various criteria that they have set for themselves from previous experiences. Unfortunately, these criteria are quite vague and operator dependent.

To eliminate the uncertainly caused by qualitative human grading, a vision based automated steel surface analysis system is desirable. Such a system should ideally be able to provide a more quantitative analysis of the steel surface roughness. Furthermore, based in these results the system should also be able to automatically classify steel samples into different grades. Such an automated steel surface analyzer leads into the realm of machine vision, which employs cameras that provide data to a computer that makes decisions based on preset criteria. The data is usually in the form of digital images. The vision system is setup in an *optimal* manner in order to capture images in such a way that they are able to provide the necessary visual information required by the computer to make decisions. In the case of steel surface pitting, it is necessary to image the surface in a way that the surface pits are adequately highlighted.

For purposes of texture analysis and automatic classification, several steel slabs with varying degrees of surface pits were cut from finished steel rolls and digitally imaged in the laboratory. However, in order to highlight the surface pits, prior to imaging, each slab was pre-treated by pouring black ink upon the surface. After the ink had filled into the pits, the steel slabs were lightly cleaned with a cloth. This resulted in the steel surface pits being represented by black spots. The stained steel slabs were then digitally imaged as grayscale images. As explained earlier, steel slab surfaces that are smooth (i.e. with good surface properties), contain randomly distributed shallow pits (i.e. dark ink spots). Figure 1(a) illustrates an example of a grayscale image of a steel slab that has good surface qualities due to the nature and distribution of surface pits. An example of a bad steel surface quality grayscale image is shown in Figure 1(b), which contains various '*snake*' like patterns representing deep pits that have joined to form craters.

Several control steel slabs of varying surface smoothness were similarly imaged after they underwent the ink pre-treatment process. These samples were also pre-analyzed by trained operators for grading the steel (based on surface roughness) and labeling each sample as good or bad surface quality. The images of these control steel samples have been used for the analyses that follow in this paper. For sake of simplicity, both in terms of analysis and understanding, the chosen steel samples only belonged to one of two extremes (i.e. good or bad steel surface quality). The two sample images illustrated in Figure 1 were used for training the PCA model used in MIA. Once trained, the model was then used for dual purposes. First, monitoring spatial locations of major surface pits in subsequent steel surface images. Second, classification of each sample into one of two classes, based on good/bad surface quality. Since all the steel samples were pre-labeled by operators, the automatic classification based on MIA could be tested to determine its accuracy. The data set used for testing the monitoring and classification schemes consisted of four pre-labeled images (2 pre-labeled images per class based on surface pitting). The testing data set images are illustrated in Figure 2(a) & (b). Each image used for training and testing the MIA model is 8-bit grayscale with pixel dimensions of 479×508 (rows $\times$ columns).

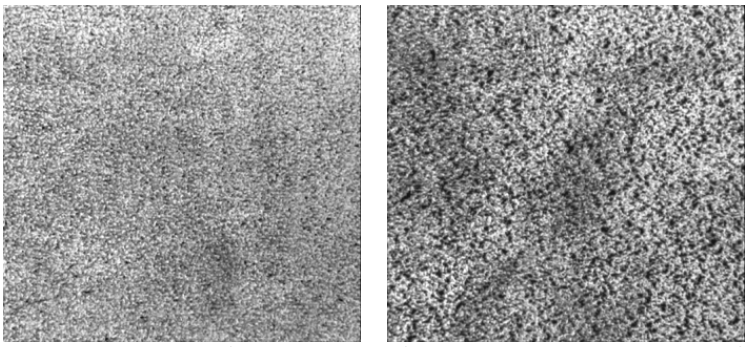

Figure 1 Training data: (a) Good quality steel surface (low degree of pitting); (b) Bad quality steel surface (high degree of pitting)

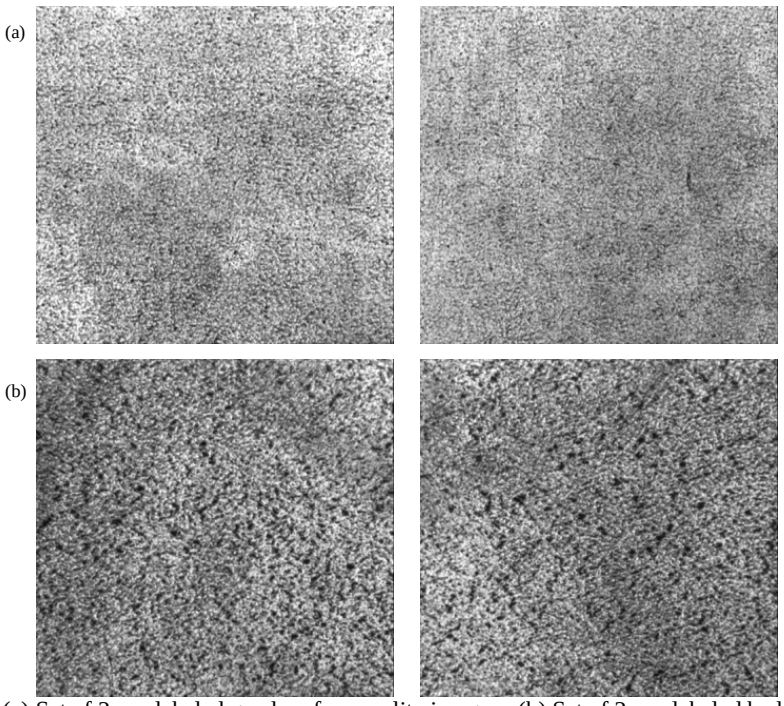

Figure 2 Test data: (a) Set of 2 pre-labeled good surface quality images; (b) Set of 2 pre-labeled bad surface quality images

2.1. Pre-processing grayscale images for MIA

Upon observing the images in Figures 1 & 2 it can be seen that the main distinguishing feature between the steel surface pits and the background pixels is a sharp change in pixel intensities at the edge of each pit. As a result, in order to create a meaningful feature-space for maximum distinction between the two classes of steel samples based on surface quality, it becomes important to enhance the spatial distribution of pit edge pixel intensities throughout the sample images. One possible technique of capturing this spatial distribution is through spatially shifting the grayscale image in adjacent directions, and then stacking the shifted images on top of each other to form a three-way pixel array. Each image in such a stack would illustrate the same feature information. However, the sharp pixel intensity changes around steel surface pits would be further enhanced in such a representation. This is because adjacent pixel information gets supplemented to every pixel in the two-dimensional image plane of the three-way array. Schematically, this information can be viewed as a vector in the variable (i.e. shifting index) dimension of the multivariate image. Figure 3(a) illustrates such a multivariate image that is created by spatially shifting an image in four adjacent directions, and stacking the shifted images on top of each other. Alternately, the same multivariate image is also illustrated in Figure 3(b) as a two-way array of variable vectors. Each variable vector in such a representation contains pixel information from a chosen neighborhood of pixels in the image depending upon the amount of shifting applied to the grayscale image. The amount (i.e. number of pixels) and direction of spatial shifting that is performed on the grayscale images is another variable that is dependent on the shapes and sizes of the major surface pits in the steel samples. Generally, enough shifting should be performed such that the edges of major pits are adequately captured upon performing MIA on the resulting multivariate image.

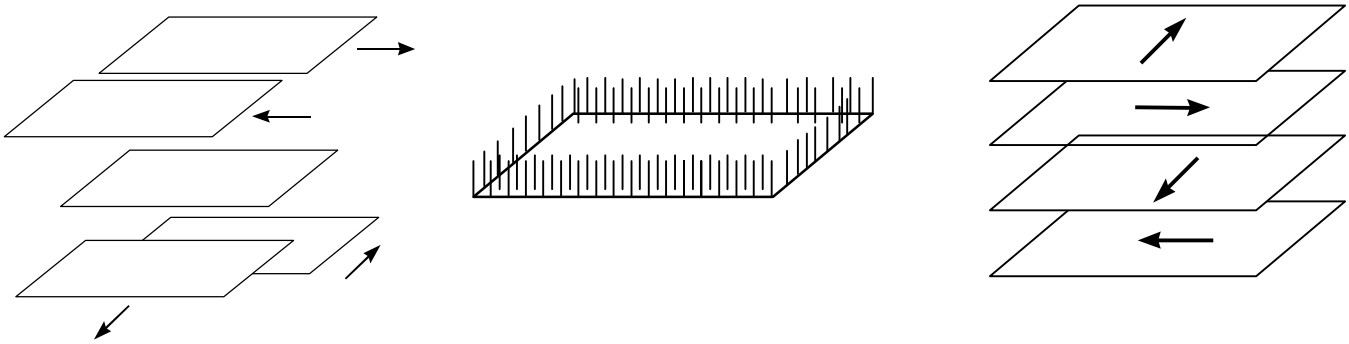

Figure 3 (a) A multivariate image created via spatial shifting in 4 adjacent directions &stacking the shifted images; (b) A multivariate image viewed as a two-way array of variable vectors orthogonal to the image plane (for graphical clarity not all variable vectors are shown); (c) A multivariate image created via rotating at right angles & stacking the rotated images

3. MIA OF SPATIALLY SHIFTED AND STACKED GRAYSCALE IMAGES

The MIA models used for further analyses were created using the training data set from Figure 1 since these images represent extreme contrasts in their surface roughness properties. Both images were shifted in 8 adjacent directions by 1 pixel as illustrated in Figure 3(a), and the shifted images were stacked to form 9 variable multivariate images, respectively. As the number of pixels by which each image is shifted increases, the variable dimension of the resulting multivariate image also increases drastically (8 extra variable images per increase in pixel shift in all adjacent directions). This also affects the computational effort required to process the multivariate image. As far as this paper is concerned each grayscale image sample is limited to a spatial shift by 1 pixel in 8 adjacent directions. After shifting and stacking the image sample the three-way array is cropped at the edges to discard all the non-overlapping sections. This results in the multivariate image having smaller image plane dimensions than those of the original image sample. In case of the training and testing images used in this paper, the dimensions of the shifted and stacked multivariate image were $477 \times 506 \times 9$. MIA was performed on both the good and bad surface property multivariate image arrays $\underline{\mathbf{X}}_{good}$ and $\underline{\mathbf{X}}_{bad}$ using multi-way PCA based on the kernel algorithm[9] to decompose the data into various Principal Components (PCs). The cumulative percent sum of squares explained by the first 3 PCs in both the good and bad surface training sample images were 99.36% and 99.20%, respectively. Hence, only the first 3 PCs have been used in subsequent analyses throughout this paper. The rest of the PCs (4 to 9) were attributed to explaining noise in the multivariate image.

Since no mean centering of the image data was performed prior to application of multi-way PCA, the first PC of both the training images explains majority of the pixel intensity variations in the image. This is evident by studying the reorganized score vector $\mathbf{t}_1$ into a two-way array $\mathbf{T}_1$ as intensity images for both training samples. Figures 4(a) and (b) illustrate $\mathbf{T}_{1good}$ and $\mathbf{T}_{1bad}$, respectively. Upon comparison of Figure 4 with the original training set images in Figure 1 it can be seen that the PC1 score images are blurred versions of the originals. This is due to the fact that PC1 extracts only the pixel contrast information from the multivariate image via averaging over the neighborhood of pixels contained in each variable vector [Figure 3(b)] of the three-way pixel array.

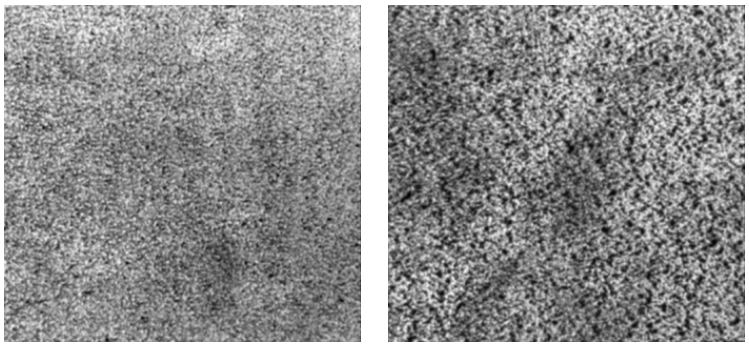

Figure 4 (a) $\mathbf{T}_1$ image of good steel surface training image; (b) $\mathbf{T}_1$ image of bad steel surface training image

Upon extracting the mean pixel intensity variations from the multivariate image, the second and third PCs of MIA extract the remaining feature information. Figure 5(a) and (b) illustrates the second PC score images $\mathbf{T}_{2good}$ and $\mathbf{T}_{2bad}$ of the good and

bad steel surface training images, respectively. A close observation of both $\mathbf{T}_2$ score images reveals that the second PC predominantly extracts horizontal edges of the surface pits in both the training set images. Furthermore, PC2 also extracts diagonal edge information in all four directions (i.e. 45°, 135°, 225°, & 315°) with respect to the center of the image.

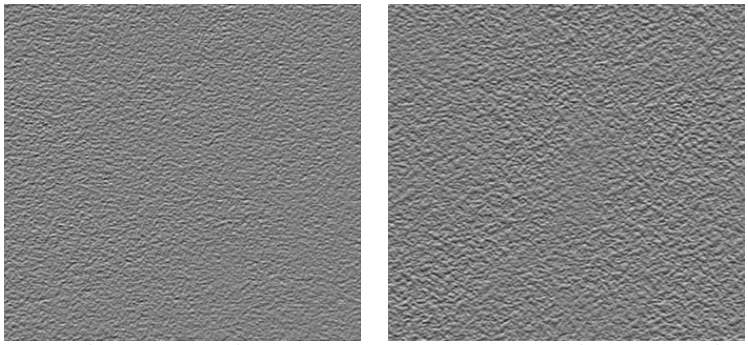

Figure 5 (a) $\mathbf{T}_2$ image of good steel surface training image; (b) $\mathbf{T}_2$ image of bad steel surface training image

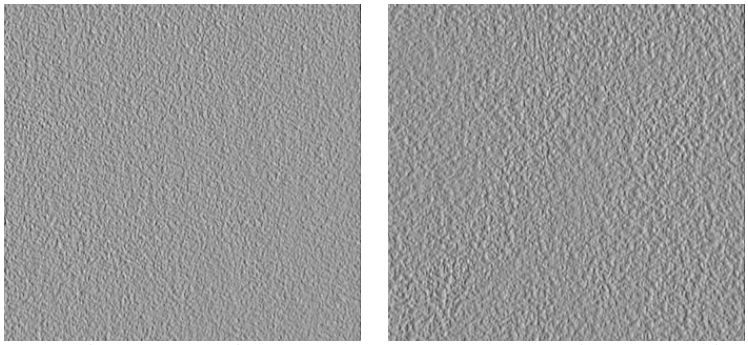

Figure 6 (a) $\mathbf{T}_3$ image of good steel surface training image; (b) $\mathbf{T}_3$ image of bad steel surface training image

The third PC score images $\mathbf{T}_{3good}$ and $\mathbf{T}_{3bad}$ of the good and bad steel surface training samples are illustrated in Figure 6(a) and (b), respectively. It can be seen from both images in Figure 6 that the main features extracted by PC3 are the vertical edges of the steel surface pits. Similar to the previous PC (i.e. $\mathbf{T}_2$) it can be seen that PC3 also extracts diagonal surface pit edge information in all four directions throughout both training images.

Observing the score images of the training data for all three PCs one can gather that in this particular case MIA serves as three different filters on the grayscale image. PC1 serves as a smoothing filter, whereas PC2 and PC3 server as 1st-derivative horizontal and vertical edge detection filters, respectively. However, generalization of MIA as simple filters for grayscale images is invalid. This is because MIA decomposes a multivariate image into a linear combination of score and loading vectors based on explanation of the maximum pixel intensity variations throughout the three-way data. It is entirely problem dependent how one wishes to arrange this three-way data for MIA. For example, multispectral images are naturally multivariate in nature. Here, wavelength serves as the variable dimension of the three-dimensional pixel array. Besides shifting/stacking, grayscale images can be represented as three-dimensional pixel data using several operations to create a meaningful variable dimension for MIA (e.g. rotation/staking images, filtering/stacking images, thresholding/stacking images at different threshold values). Figure 3(c) illustrates one such alternate representation of a multivariate image created by rotating a grayscale image at right angles (i.e. 0°, 90°, 180°, & 270°) with respect to its center, and stacking the rotated images to form a three-way array. The shifting/stacking operation described in this paper was purposely used to extract texture/roughness information using the advantageous features of MIA from the grayscale image. However, no a priori information was supplied to MIA as the grayscale image was shifted by an equal number of pixels in all adjacent directions to form the three-way data. As a result, the decomposition was unbiased, and the LV space of MIA extracted relevant feature information from the three-dimensional image stack in the first three PCs.

Besides providing the user with a visual analysis of the LV scores through intensity images (i.e. image space), MIA has the added advantage of letting the user observe pairs (or triplets) of score vectors through scatter plots (i.e. score space). The score vectors ($\mathbf{t}_1$, $\mathbf{t}_2$, …) of the dominant PCs of the multivariate image summarize feature information via point clusters in the score space of MIA. If, at different pixel locations in an image, the same feature is present (e.g. steel surface pits), the score value combination (t_1, t_2) of this feature in the score space would be similar for these pixels. Upon scatter plotting the score vectors (e.g. $\mathbf{t}_1$ vs. $\mathbf{t}_2$) those pixels belonging to similar features, regardless of their spatial locations throughout the

image, would fall in the same region of the score plots. This results in point clusters that represent unique features. Since similar score combinations would result in scatter plots having points falling on top of each other, one can use score plots with pixel densities (i.e. number of points that are on top of each other at a particular location) to determine the score concentrations. Score values that have a high pixel density would form a brighter point cluster in the score space. Figure 7(a) and (b) illustrates the score space of the first two PCs (i.e. $\mathbf{t}_1$ vs. $\mathbf{t}_2$) of the good and bad steel surface training images, respectively. It can be seen from both score plots in Figure 7 that majority of the scores form one big point cluster in the middle of the plot. This pattern is due to the fact that the multivariate image was formed using the same image shifted and stacked on top of each other. As a result, it would be expected that majority of the information in the central point cluster represents average pixel contrast through the images. Similar cluster patterns can also be noticed in the PC23 score plots (i.e. $\mathbf{t}_2$ vs. $\mathbf{t}_3$) of the steel surface training images. These plots are illustrated in Figure 8(a) and (b) for the good and bad steel surface training images, respectively.

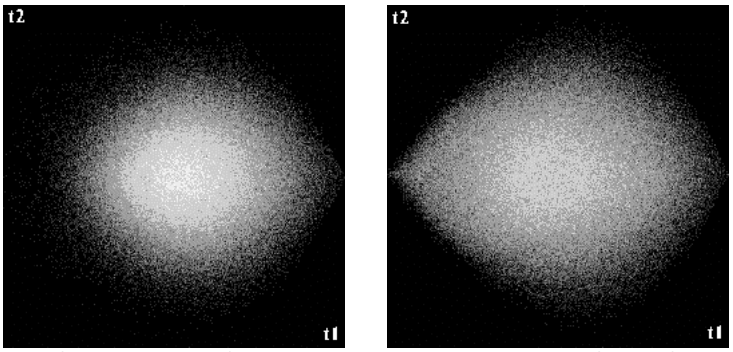

Figure 7 (a) Score space of PC12 for good steel surface training image; (b) Score space of PC12 for bad steel surface training image

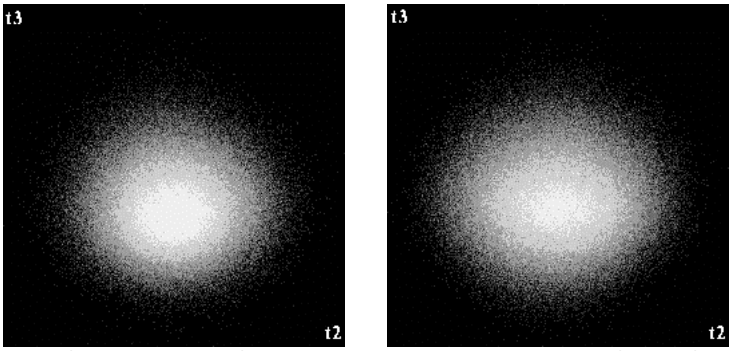

Figure 8 (a) Score space of PC23 for good steel surface training image; (b) Score space of PC23 for bad steel surface training image

In order to gain further insight about the information being decomposed into score plots one can interrogate the point clusters using various strategies. One popular technique of interrogating the information contained in the score space is via manually masking[6, 7, 10] the point clusters and highlighting the masked points as pixels in the corresponding score image. Using this procedure one can isolate those pixels belonging to a particular feature of interest via fine-tuning the mask shape and size. A close inspection of the PC1 score images in Figure 4 reveals that pixels belonging to steel surface pit cores are represented by dark shades (i.e. low pixel intensities). As a result, one can infer that the corresponding $\mathbf{t}_1$ values of these pixels would be low. One can confirm this intuition upon masking the low $\mathbf{t}_1$ values (regardless of $\mathbf{t}_2$) in the corresponding $\mathbf{t}_1$ vs. $\mathbf{t}_2$ score space. Figure 9(a) illustrates such a mask (shown as a dark-gray rectangle) that interrogates low $\mathbf{t}_1$ values without giving any preference to $\mathbf{t}_2$ in the PC12 score plot of the bad steel surface training image. The corresponding pixels that are masked in Figure 9(a) have been highlighted and overlaid on the $\mathbf{T}_1$ image of the bad steel surface training sample in Figure 9(b). Similar masking/highlighting can also be performed on the good surface training image.

Inspecting Figures 5(b) and 6(b), it can be inferred that both low as well as high pixel intensity values of $\mathbf{T}_2$ and $\mathbf{T}_3$ represent those pixels belonging to steel surface pit edges in all eight adjacent directions (horizontal & diagonal in $\mathbf{T}_2$, vertical and diagonal in $\mathbf{T}_3$). As a result, the corresponding mask that highlights pit edges in the training image data ignores the central point cluster in the $\mathbf{t}_2$ vs. $\mathbf{t}_3$ score plot. Figure 10(a) illustrates such a mask (shown in dark-gray around the central cluster) that highlights the extreme (t_2, t_3) score combinations in the $\mathbf{t}_2$ vs. $\mathbf{t}_3$ score plot of the bad surface training sample. The corresponding pixels covered by this mask have been highlighted and overlaid on the $\mathbf{T}_1$ image of the bad surface training sample in Figure 10(b). Similar results can also be obtained to highlight surface pit edges in the good steel surface training image.

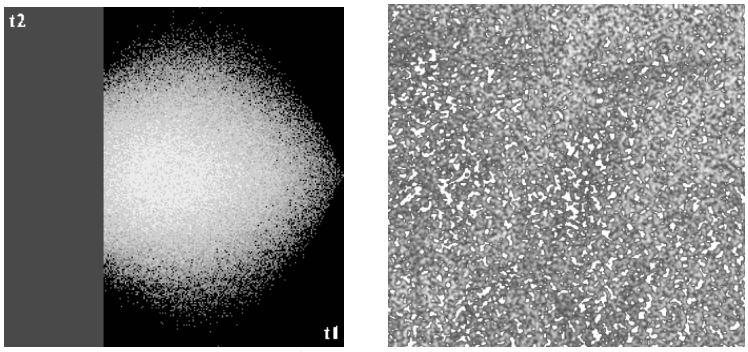

Figure 9 (a) Manually applied mask on PC12 score space of bad steel surface training image; (b) Corresponding feature pixels under PC12 mask highlighted (in white) and overlaid on $\mathbf{T}_1$ image of bad steel surface training sample image

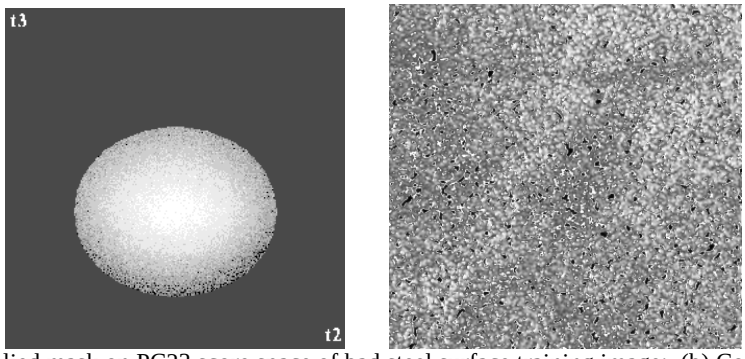

Figure 10 (a) Manually applied mask on PC23 score space of bad steel surface training image; (b) Corresponding feature pixels under PC23 mask highlighted (in white) and overlaid on $\mathbf{T}_1$ image of bad steel surface training sample image

Information gathered from MIA of the bad surface training image score and image spaces reveals the ability of multi-way PCA to extract relevant texture information from grayscale images. Once trained, the MIA models can then be used to extract similar texture properties from other steel surface grayscale images. This can be accomplished by using some of the ideas developed from the on-line monitoring aspects of MIA[11]. Without going into details this paper only describes the main ideas of the MIA monitoring approach as follows. After training the MIA model using multi-way PCA on shifted/stacked grayscale images to develop score space masks that adequately represent features of interest, one can then use the masks on the score space of the subsequent test images. Each new grayscale image undergoes the same shifting/stacking procedure, which is followed by extraction of its score space through the following equation:

$$\mathbf{t}_{a,new} = \underline{\mathbf{X}}_{new} \cdot \mathbf{p}_{a,training} \tag{2}$$

Using the new score vectors, the pixel densities in the score space of the new images can be updated. With each new image the score space point cluster patterns would change. This change would depend upon the overall features in the new image. By monitoring the changing score point pixel densities under the training masks in the score space of the new images one can track the severity of surface pits through the new steel samples. Furthermore, one can also count the number of pixels belonging to surface pit cores and their edges in the new images upon counting the number of score points that fall under the masks in the score space. Thus, a more objective measure of the steel surface pits in the new images could be obtained. Tolerance limits could be set on the number of maximum acceptable pixels belonging to steel surface pits. Upon violation of these limits, the sample under question may be further investigated by highlighting the corresponding pixels falling under the score space masks in the image space to locate the actual spatial locations of the surface pits.

4. AUTOMATIC CLASSIFICATION OF INDUSTRIAL GRAYSCALE IMAGES USING MIA

It has been discussed earlier that MIA techniques decompose the feature information from a multivariate image (whether true or created via some pre-processing) into a linear combination of score and loading vectors. These latent variables (or PCs) can be analyzed as score point scatter plots or score intensity images. Furthermore, it has also been shown that the score spaces decompose all pixels belonging to similar features into point clusters in the scatter plots. Thus, the score space of a multivariate image contains the same amount of feature information, as does its image space. However, advantage of the score space lies in its ability to break the spatial dependence of the feature pixels from the image. The score space is independent of the spatial locations of the feature pixels in the image space. This fact can be used to compare two

incongruent images that contain similar amounts of feature information in them. Various techniques can be used to compare the score spaces of the two incongruent images to determine their degree of similarity.

A two-step procedure could be employed to accomplish this task. First, one would develop latent variable score spaces for both images in question. This would be followed by comparison of the score spaces by some form of quantitative similarity measure [e.g. (i) Sum of squared differences at each location in the score plots, (ii) Straightforward regression between the two arrays, or (iii) Constructing a difference image to highlight the areas where dissimilarity is significant].

As part of the first step in this procedure one needs to perform a multi-way PCA decomposition on the training image in order to develop a representative LV model that accounts for all the feature information. This decomposition summarizes the feature information from the training image into a few score vectors. Once the multi-way PCA decomposition is complete, the resulting score space could then be used as a summarized image, where all feature information is collected in specific regions of the plots. The theory of MIA proves that all multivariate images containing similar features (regardless of their spatial locations in the scene) would produce similar score point cluster patterns[7].

The second step in this procedure includes individually comparing the point cluster patterns in the score spaces of the testing and training samples. This procedure can be termed 'template matching' since one is trying to match particular score spaces (depicted by point cluster patterns in a 2-D plot). One possible method to execute the template matching procedure would be a simple distance measure to compare similarity between two score spaces. One could calculate the sum of squared differences between score points in various bins from specific regions (representing the features of interest) in the two score spaces. Alternatively, if one requires an overall measure of similarity between the two score spaces, the sum of squared differences (SSD) could be calculated over the entire score space. This idea has been used as the main classification tool in this paper. Score plots of the two steel surface quality (good & bad) training images (Figure 1) were compared with those obtained from the four test images (Figure 2). A separate multi-way PCA analysis was performed on each training steel surface image from Figure 1 after undergoing the shifting/stacking steps described in sub-section 2.1. Both training models (one for good & one for bad steel surface quality) were used to calculate the score vectors for all four testing images from Figure 2 using Equation 2. The testing images were also pre-processed using the same shifting/stacking procedure prior to application of the two training models. Therefore, each test image from Figure 2 had two PC12, PC13, and PC23 score plots (a set of two score plots per PCA training model used). These score plots of the testing images were then compared to the respective score plots of the good or bad surface training images. For example, the good surface training image PC12 score plot [Figure 6(a)] was compared with the $PC12_{test}$ score plots (via good surface $PCA_{training}$ model) of each of the four testing images. This resulted in each test image having a set of two SSD measurements when the comparisons were complete. The training sample comparison that produced the lower of the two *mean* SSD measurements for all three score plots (i.e. PC12, PC13, & PC23) of a test image was deemed to be its correct class. Since the four test image samples had been pre-labeled by operators, it was thus easy to determine whether the classification passed or failed. The results obtained for the classification of the four test image samples are provided in Table 1.

Table 1 Classification of Steel Surface Test Images Using Mean SSD Between Candidate & Training Image MIA Score Spaces

		SSD b/w candidate and *Good Surface* Training Score Space				SSD b/w candidate and *Bad Surface* Training Score Space				
Candidate Image ID	Pre-Labeled Class of Candidate	PC12	PC13	PC23	**Mean SSD**	PC12	PC13	PC23	**Mean SSD**	**Classification**
Fig 2(a) L	Good Surface	7.9580e07	1.1075e08	9.4515e07	**9.4948e07**	1.2338e08	1.2443e08	8.0366e07	1.0939e08	***Good Surface***
Fig 2(a) R	Good Surface	6.8788e07	1.0118e08	8.9862e07	**8.6610e07**	1.1849e08	1.2364e08	8.5950e07	1.0936e08	***Good Surface***
Fig 2(b) L	Bad Surface	1.0965e08	9.4741e07	6.3388e07	8.9260e07	6.9297e07	6.7300e07	6.1087e07	**6.5895e07**	***Bad Surface***
Fig 2(b) R	Bad Surface	1.2269e08	9.5471e07	6.8516e07	9.5559e07	7.3766e07	7.7148e07	6.8797e07	**7.3237e07**	***Bad Surface***

It can be seen from the above table that all four test images were correctly classified into their pre-labeled classes. Thus, the idea of classifying grayscale images based on SSD measurements between their MIA score spaces shows promise. However, SSD measurements are only one of the possible techniques of comparing/classifying images based on score plot pattern matching. A simple regression model between the two score spaces to determine their overall similarity could also be used as an alternative method. In this case one can use a pixel-to-pixel matching regression function between the two score spaces. Theoretically, as long as the *total* pixels that belong to all the features in both images are comparable, the corresponding score point clusters of both score spaces should exhibit similar patterns in order to produce significant regression parameters.

5. CONCLUSIONS

In this paper we have explored the potential of applying a new multivariate statistical texture analysis method using Multivariate Image Analysis techniques based on multi-way PCA to extract surface roughness information from grayscale images. Since MIA techniques are ideally suited for analyzing multivariate image data, direct application of these techniques on grayscale images is not possible. This is because grayscale image data is two-dimensional in nature as opposed to multi-dimensional data present in multivariate images. Prior to applying MIA for texture analysis, this paper introduces a novel technique of logically creating a 3rd dimension to enhance surface roughness features in grayscale images by complementing its two-way pixel array. This is accomplished via: first, spatially shifting the image in adjacent directions; second, stacking the shifted images on top of each other; and finally, cropping the non-overlapping sections from the edges of the three-way array. MIA techniques can then be applied on the resulting multivariate image where the third (i.e. variable) dimension serves as the spatial shifting index.

Several image samples representing one of two grades of steel surfaces were used to test the application of MIA techniques on grayscale images for purposes of texture analysis and automatic classification. The steel samples were pre-graded by trained operators based on surface roughness criteria mainly characterized by pit formation. Multi-way PCA was used to decompose the shifted/stacked grayscale images into linear combinations of score and loading vectors. The resulting MIA image space revealed that PC1 mainly extracted overall pixel contrast information, whereas PC2 and PC3 extracted edge information of the steel surface pits. Thus, the MIA image space served as a smoothing filter in the first latent variable, and a 1st-derivative edge enhancement filter in both the second and third latent variables. This was expected since the grayscale images were pre-processed in order to enable MIA techniques to extract texture information. The steel surface feature information was also captured in the MIA score space via scatter plots of PC12 and PC23 score vectors. The point cluster patterns were interrogated using manually applied masks and highlighting the corresponding pixels in the MIA score images. These masks captured pixels belonging to steel surface pit cores and edges in the steel surface images. The trained MIA model that captures surface texture properties of the steel images can subsequently be used to identify and monitor similar feature pixels from images of other steel surface images. Finally, the texture analysis properties of MIA were used to illustrate an automatic steel surface image classification technique. The classification criteria used were the steel surface texture properties (i.e. pit cores and edges) in the candidate images. MIA score plot cluster patterns were used as the main tools in this classification scheme. Since score plots compress all feature information from a multivariate image into a point cluster pattern, it is expected that two incongruent images possessing similar overall feature characteristics (in terms of number of pixels per feature) would collapse into similar score patterns. Using various techniques of measuring the similarities (local or global) between score plots of two images, one can quantitatively classify various image samples into pre-defined classes. In case of the steel surface images, samples were classified into one of two possible classes based on severity of surface pitting. The mean sum of squared differences over the entire score plots of two images was calculated to determine a quantitative measure of similarity. Classification using this technique correctly grouped four pre-labeled test sample images into their respective classes.

Based on some of the results obtained in this paper it can be shown that (after some pre-processing) multivariate statistical texture analysis techniques can be successfully applied to extract surface feature information from grayscale images. One of the main advantages of the proposed methodology is its ability to also be directly applicable to color, as well as naturally multivariate (e.g. multispectral) image data. Using LV score and image spaces these methods break the spatial dependence of image pixels belonging to surface texture characteristics. The corresponding LV spaces can then be used to both detect as well as monitor future occurrences of similar texture feature pixels in subsequent images. As a result, this strategy also opens the doors to possible applications in off-line quality control, or on-line feedback control of vision based industrial processes that are being monitored using digital cameras.

REFERENCES

1. R. C. Gonzalez, P. Wintz, *Digital Image Processing, 2nd ed.*, Addison-Wesley, Reading, 1987.
2. W. K. Pratt, *Digital Image Processing*, John Wiley & Sons, New York, 1978.
3. J. C. Russ, *The Image Processing Handbook*, CRC Press, Boca Raton, 1992.
4. F. Tomita, S. Tsuji, *Computer Analysis of Visual Textures*, Kulwer Academic, Boston, 1990.
5. P. Geladi, H. Isaksson, L. Lindqvist, S. Wold, K. Esbensen, "Principal Component Analysis of Multivariate Images," *Chem. And Int. Lab. Sys.* **5**, pp. 209-220, 1989.
6. K. Esbensen, P. Geladi, "Strategy of Multivariate Image Analysis (MIA)," *Chem. And Int. Lab. Sys.* **7**, pp. 67-86, 1989.

7. P. Geladi, H. Grahn, *Multivariate Image Analysis*, John Wiley & Sons, Chichester, 1996.
8. J. F. MacGregor, M. H. Bharati, H. Yu, "Multivariate image analysis for process monitoring and control," Presented at SPIE Symposium on Intelligent Systems and Advanced Manufacturing, *Proceedings of SPIE*, **4188**, Boston, 2000.
9. F. Lindgren, P. Geladi, S. Wold, "The Kernel Algorithm for PLS," *J. Chemometrics* **7**, pp. 45-59, 1993.
10. M. H. Bharati, J. F. MacGregor, "Multivariate Image Analysis for Real-Time Process Monitoring," *Ind. Eng. Chem. Res.* **37**, pp. 4715-4724, 1998.
11. M. H. Bharati, "Multivariate Image Analysis for Real-Time Process Monitoring and Control," M. Eng. Thesis, McMaster University, Hamilton, 1997.